Glycosylphosphatidylinositol anchors regulate glycosphingolipid levels.

Loizides-Mangold, Ursula ; David, Fabrice P A ; Nesatyy, Victor J ; Kinoshita, Taroh ; Riezman, Howard

Abstract: Glycosylphosphatidylinositol (GPI) anchor biosynthesis takes place in the endoplasmic reticulum (ER). After protein attachment, the GPI anchor is transported to the Golgi where it undergoes fatty acid remodeling. The ER exit of GPI-anchored proteins is controlled by glycan remodeling and p24 complexes act as cargo receptors for GPI anchor sorting into COPII vesicles. In this study, we have characterized the lipid profile of mammalian cell lines that have a defect in GPI anchor biosynthesis. Depending on which step of GPI anchor biosynthesis the cells were defective, we observed sphingolipid changes predominantly for very long chain monoglycosylated ceramides (HexCer). We found that the structure of the GPI anchor plays an important role in the control of HexCer levels. GPI anchor-deficient cells that generate short truncated GPI anchor intermediates showed a decrease in very long chain HexCer levels. Cells that synthesize GPI anchors but have a defect in GPI anchor remodeling in the ER have a general increase in HexCer levels. GPI-transamidase-deficient cells that produce no GPI-anchored proteins but generate complete free GPI anchors had unchanged levels of HexCer. In contrast, sphingomyelin levels were mostly unaffected. We therefore propose a model in which the transport of very long chain ceramide from the ER to Golgi is regulated by the transport of GPI anchor molecules.

DOI: https://doi.org/10.1194/jlr.M025692

GPI anchors regulate glycosphingolipid levels

Ursula Loizides-Mangold[1], Fabrice P.A. David[2], Victor J. Nesatyy[2], Taroh Kinoshita[3] and Howard Riezman[1]

[1]Department of Biochemistry, NCCR Chemical Biology, University of Geneva, CH-1211 Geneva, Switzerland
[2]Global Health Institute, Ecole Polytechnique Fédérale de Lausanne, Faculty of Life Sciences, Lausanne, Switzerland
[3]Research Institute for Microbial Diseases and WPI Immunology Frontier Research Center, Osaka University, Suita, Osaka 565-0871, Japan

Running title: Lipidomic profile of GPI anchor deficient cells

Abbreviations: CE, cholesterol ester; Cer, ceramide; EtN-P, ethanolamine-phosphate; GlcCer, glucosylceramide; GPI, glycosylphosphatidylinositol; HexCer, hexylceramide; PC, phosphatidylcholine; PE phosphatidylethanolamine; PI, phosphatidylinositol; PS, phosphatidylserine; SM, sphingomyelin

Address correspondence to:
Howard Riezman, Ph.D.
University of Geneva, Department of Biochemistry,
30 Quai Ernest-Ansermet
CH-1211 Geneva, Switzerland
Phone: +41 (22) 379-6469
Fax: +41(22) 379-6470
email: howard.riezman@unige.ch

Abstract

Glycosylphosphatidylinositol (GPI) anchor biosynthesis takes place in the endoplasmic reticulum (ER). After protein attachment the GPI anchor is transported to the Golgi where it undergoes fatty acid remodeling. The ER exit of GPI anchored proteins is controlled by glycan remodeling and p24 complexes act as cargo receptors for GPI anchor sorting into COPII vesicles. In this study, we have characterized the lipid profile of mammalian cell lines that have a defect in GPI anchor biosynthesis. Depending on which step of GPI anchor biosynthesis the cells were defective we observed sphingolipid changes predominantly for very long chain monoglycosylated ceramides (HexCer). We found that the structure of the GPI anchor plays an important role in the control of HexCer levels. GPI anchor deficient cells that generate short truncated GPI anchor intermediates showed a decrease in very long chain HexCer levels. Cells that synthesize GPI anchors but have a defect in GPI anchor remodeling in the ER have a general increase in HexCer levels. GPI-transamidase deficient cells that produce no GPI anchored proteins, but generate complete free GPI anchors had unchanged levels of HexCer. In contrast, sphingomyelin levels were mostly unaffected. We therefore propose a model in which the transport of very long chain ceramide from the ER to Golgi is regulated by the transport of GPI anchor molecules.

Introduction

Lipid anchoring of proteins to the outer leaflet of the plasma membrane is essential for cellular function and development (1). One prominent lipid anchor is a complex glycolipid called glycosylphosphatidylinositol (GPI). The GPI anchor has the core structure phosphatidylinositol (PI) – glucosamine (GlcN) – $(Mannose)_3$ – phosphoethanolamine (EtN-P) which is conserved among all species. After biosynthesis the GPI-anchor is attached post-translationally to the newly generated C-terminus of certain eukaryotic proteins destined for anchoring thereby tethering the protein to the membrane surface by the glycolipid moiety. GPI-anchored proteins can be released from the cell surface by phosphatidylinositol specific phospholipases and this cleavage event can induce major conformational changes on the GPI-anchored protein itself (2).

At least three organelles, endoplasmic reticulum (ER), Golgi and peroxisomes are involved in the biosynthesis and remodeling of the GPI anchor. The biosynthesis is initiated on the outer side of the endoplasmic reticulum membrane. After the first two reactions the GPI-anchor precursor is flipped and biosynthesis continues on the luminal side of the ER where the diacyl chains of phosphatidylinositol are then replaced by alkyl-acyl chains. This step is impaired in mutants of the peroxisomal alkyl phospholipid biosynthesis pathway (3).

After protein attachment, the GPI anchor undergoes complex remodeling that begins in the ER with the removal of the inositol–linked acyl chain (4) and the remodeling of the GPI glycan part (5). Glycan remodeling is crucial for sorting of GPI anchored proteins into ER exit sites and their subsequent ER to Golgi transport (6). In mammalian cells remodeling of the GPI anchor is then continued in the Golgi where the unsaturated fatty acid of the GPI anchor is replaced by a saturated fatty acid chain (7). From the Golgi compartment, GPI-anchored proteins are transported to the plasma membrane where they are thought to associate preferentially with

glycosphingolipids and cholesterol to be enriched in lipid ordered microdomains. Lipid remodeling is likely to be important for this association because unremodeled GPI-anchored proteins, which carry unsaturated fatty acids, are no longer enriched in detergent resistant membrane fractions (7). Treatments that deplete either membrane cholesterol or sphingolipids also disrupt the association of GPI anchored proteins with detergent-resistant membranes (DRMs) further supporting the notion that specialized domains are critical for the correct localization of this subset of proteins (8, 9).

Importantly, trafficking of GPI anchored proteins is affected by alterations in sphingolipids and sterols. In yeast, the ER to Golgi transport of GPI anchored proteins is rapidly reduced by inhibition of *de novo* sphingolipid biosynthesis without affecting the transport of soluble or transmembrane proteins (10, 11). However, GPI anchored proteins might play an important role in the transport of membrane proteins such as Tat2 and Fur4p which are no longer associated with DRMs and are retained in the ER in *v* cells that are deficient at an early stage of GPI anchor biosynthesis (12). In mammalian cells it was shown that inhibition of sphingolipid biosynthesis affects apical targeting of GPI-anchored proteins in Madin-Darby canine kidney (MDCK) cells (13) and sorting of the axonal GPI-anchored protein Thy-1 in primary hippocampal neurons (14). However unlike yeast, ER-to-Golgi transport of GPI-APs in mammalian cells does not depend on *de novo* sphingolipid biosynthesis (15).

An important characteristic of sphingolipid trafficking is the coexistence of at least two different ceramide transport pathways, a major ATP and cytosol dependent pathway and a minor ATP or cytosol-independent pathway (16). Evidence for two different ceramide transport pathways was first obtained with the isolation of the CHO mutant cell line LY-A that shows a defect in sphingomyelin but not in HexCer biosynthesis (17) and the subsequent identification of a

ceramide transport protein called CERT (18). Two pathways for ceramide transport also exist in yeast (19).

As changes in lipid composition affect GPI anchored proteins, we asked whether a lack of GPI-anchored proteins together with the abnormal accumulation of GPI-anchor intermediates would affect the lipid profile of mammalian cells. To address this question, we made use of a series of mutant Chinese hamster ovary (CHO) cell lines (1) that have defects along the GPI-anchor biosynthesis pathway. We determined the lipid profile of the GPI anchor deficient cells using a lipidomics approach. Lipidomics has emerged in the era of genomics and proteomics as a rapidly expanding research field due to recent advances in mass spectrometry and bioinformatics. Here, we applied tandem mass spectrometry coupled with multiple reaction monitoring (MRM) to detect and quantify over 850 phospho- and sphingolipids from GPI anchor deficient cells. Using the same crude lipid extracts, we analyzed complex glycosphingolipids by a non-targeted mass spectrometry approach and also investigated the sterol composition of each sample by GC-MS.

Materials and Methods

Chemicals and lipid standards

DLPC 12:0/12:0 (850335), PE 17:0/14:1 (PE31:1, LM-1104), PI 17:0/14:1 (PI31:1, LM-1504), PS 17:0/14:1 (PS31:1, LM-1304), C17:0 ceramide (860517), C12:0 SM (860583) and Glucosyl C8:0 Cer (860540) were used as internal lipid standards and were purchased from Avanti Polar Lipids Inc (Alabaster, Alabama, USA). Ergosterol was used as sterol standard and was purchased from Fluka (Buchs, Switzerland).

Methyl *tert*-butyl ether (MTBE) was from Fluka (Buchs). Methylamine (33% in absolute ethanol) was from Sigma Aldrich (Steinheim, Germany). HPLC grade chloroform was purchased from Acros (Geel, Belgium), LC-MS grade methanol and LC-MS grade ammonium acetate were from Fluka. LC-MS grade water was purchased from Biosolve (Valkenswaard, Netherlands).

Cell culture and transfection

All CHO cell lines used in this study were from the laboratory of Taroh Kinoshita (1). Cells of the F21 background stably express the GPI anchor marker proteins CD59 and DAF and twelve proteins involved in GPI anchor biosynthesis (20) whereas cells of the C311 background express four proteins of the GPI anchor biosynthesis pathway in addition to the markers CD59 and DAF (21-23). Presence of those plasmids was verified by antibiotic resistance of cells to G418, hygromycin B and blasticidin S (F21 series) or resistance of cells to G418, hygromycin B and puromycin (C311 series). For lipid extraction, cells were maintained in Ham's F-12 medium (Invitrogen) supplemented with 10 % fetal calf serum (FCS) and 1 % PS (penicillin (50 U/ml) and streptomycin (50 U/ml), Invitrogen). HeLa cells were maintained in DMEM (Invitrogen) with 10 % FCS supplemented with 1 % PS. All cells were grown at 37 °C and 5 % CO_2.

HeLa cells were transiently transfected with siRNA using Lipofectamine RNAiMAX (Invitrogen) according to the manufacturer's instructions. Human ON-TARGETplus SMARTpool siRNA for PIG-L (L-011953-01-0005), DPM3 (L-017492-02-0005), PIG-X (L-013784-02-0005), PIG-F (L-011753-01-0005), PIG-O (L-008728-01-0005), PIG-U (L-017428-00-0005), PGAP1 (L-008110-01-0005), PGAP5 (L-008547-01-0005), p23 (L-003718-00-0005), p24 (L-008074-01-0005), CERT (L-012101-00-0005) and control scrambled siRNA (ON-

TARGETplus non-targeting Pool D-001810-10-05) were purchased from Thermo Scientific. GeneSolution siRNA against PGAP2 (1027416) was purchased from Qiagen.

Stable CHO transfectants expressing human PIG-F or PIG-U respectively together with the Venus-FLAG-CD59 construct were established by transfection with Lipofectamine 2000 (Invitrogen) followed by selection with Zeocin (300 μg/ml, Invitrogen) for two weeks. Single clones were isolated, expanded and analyzed for CD59-Venus surface expression as a marker for restored GPI anchor biosynthesis.

Plasmids

Using the EcoRI / NotI restriction sites human PIG-F and PIG-U were subcloned from pMEori-PIG-F and pME-PIG-U (20) into the pcDNA^{TM}3.1/Zeo$^{(+)}$ mammalian expression vector (Invitrogen). Constructs were verified by sequencing. Vector pME-puro-Venus-FLAG-CD59 (15) was obtained from the laboratory of Reika Watanabe (University of Geneva, Switzerland).

RNA isolation and quantitative RT-PCR

Total RNA was isolated from HeLa cells 72 h after transfection using the RNeasy MINI kit (Qiagen) according to the manufacturer's instructions. RNA was converted into cDNA using random hexamers and Superscript II reverse transcriptase (Invitrogen). qRT-PCR was carried out on a BIO-RAD iCycler machine (BioRad, Hercules, CA, USA) with the ABsolute^{TM}QPCR SYBR Green reagent (Thermo Scientific). Results were normalized against *TBP* expression. All primers except for PIG-U, PGAP1 and PGAP5 were designed using the NCBI Primer BLAST web tool. The following primer were used: PIGL.For 5'-GGGTGCTCTGTGCTCACGCT-3', PIGL.Rev 5'-TGGCTTTCTTGGCCTGTGCCA-3'; DPM3.For 5'-

GGCCACTGCCCGCCTACTTG-3', DPM3.Rev 5'-GTCGGCTCGGGCCTCCTGTA-3'; PIGX.For 5'-GCTCTGACGCCGGCATAAGGG-3', PIGX.Rev 5'-GACGGCAGGTGTGCAAGTCCTC-3'; PIGF.For 5'-GCCGCCCGTCGTACCTGATG-3', PIGF.Rev 5'-TGGCTAGCTAACTCTCCCTCCCG-3'; PIGO.For 5'-CACCACCATGCAGCGCCTCA-3', PIGO.Rev 5'-CGCCTTCCTGCACTGGTGAGC-3'; PGAP2.For 5'-GCTGGAGTGTACACCATCTTTGCC-3', PGAP2.Rev 5'-CCGAAGTCCCACCAGGCCGT-3'; CERT.For 5'-AGGCTGTCATCACACCTCACGA-3', CERT.Rev 5'-AGCCATGTCGACGCAAGCTGG-3'; p23.For 5'-TGCGCAGCCACCTCAAGATCAC-3', p23.Rev 5'-CGCCCTGTTCCCTTGCTCTCA-3'; p24.For 5'-TCGACGTGGAGATTACAGGACCA-3', p24.Rev 5'-TGGAGTCATGGTGGACATCCGGT-3'; TBP.For 5'-CCGAATATAATCCCAAGCGGT-3', TBP.Rev 5' AAATCAGTGCCGTGGTTCGT-3'. For PIG-U, PGAP1 and PGAP5 pre-designed primersets from Qiagen (QuantiTect Primer Assay) were purchased. Relative CHOP and BiP mRNA levels were measured against TBP expression by qRT-PCR using primer: CHOP.For 5'-AGAACCAGGAAACGGAAACAGA-3'; CHOP.Rev 5'-TCTCCTTCATGCGCTGCTTT-3'; BiP.For 5'-TGTTCAACCAATTATCAGCAAACTC-3'; BiP.Rev 5'-TTCTGCTGTATCCTCTTCACCAGT-3' (24). The efficiency of each primer set was determined to be between 90-100 %.

Lipid extraction protocols

Lipid extracts were prepared using the MTBE protocol (25). Briefly, 2.5 x 10^6 cells were resuspended in 100 µl H_2O. The cell suspension was transferred into a 2 ml Eppendorf tube. 360 µl methanol and a mix of internal standards was added (400 pmol DLPC, 1000 pmol

PE31:1, 1000 pmol PI31:1, 3300 pmol PS31:1, 2500 pmol C12SM, 500 pmol C17Cer and 100 pmol C8GC). Samples were vortexed and 1.2 ml of MTBE was added. Samples were placed for 10 min on a multitube vortexer at 4 °C (Lab-tek International, Christchurch, New Zealand) followed by an incubation for 1h at room temperature (RT) on a shaker. Phase separation was induced by addition of 200 µl MS-grade water. After 10 min of incubation at RT samples were centrifuged at 1000 g for 10 min. The upper (organic) phase was transferred into a 13 mm glass tube (Corning) with a Teflon-lined cap and the lower phase was re-extracted with 400 µl of a MTBE/MeOH/H_2O mixture (10:3:1.5). Samples were vortexed, incubated for 10 min at RT and centrifuged for 10 min at 1000 g. The upper phase was collected and the combined organic phases were dried in a CentriVap Vacuum Concentrator (Labconco, MO, USA). In total 1500 µl of organic phase was recovered from each samples and split into three parts. One part was treated by alkaline hydrolysis to enrich for sphingolipids and the other two aliquots were used for glycerophospholipid and sterol analysis, respectively.

Glycerophospholipids were deacylated according to the method by Clarke (26). Briefly, 1 ml freshly prepared monomethylamine reagent (methylamine/H_2O/*n*-butanol/methanol at 5/3/1/4 (vol/vol)) was added to the dried lipid extract and then incubated at 53 °C for 1 h in a water bath. Lipids were cooled to RT and then dried in a CentriVap Vacuum Concentrator. For desalting, the dried lipid extracts were resuspended in 300 µl water-saturated *n*-butanol. The extracts were sonicated and then extracted with 150 µl H_2O. The organic phase was collected, and the aqueous phase was re-c xextracted twice with 300 µl water-saturated *n*-butanol. The organic phases were pooled and dried in a CentriVap Vacuum Concentrator.

Determination of total phosphorus

The dried glycerophospholipid extract was resuspended in 250 µl chloroform/methanol (1:1) and 100 µl were placed into a 13 mm disposable pyrex tube. The solvent was completely evaporated to avoid inhibition of the reaction by organic solvents. 0, 2, 5, 10, 20 µl of a 3 mM KH_2PO_4 standard solution were placed into separate pyrex tubes. To each tube 20 µl of water and 140 µl of 70 % perchloric acid were added. Tubes were heated at 180 °C for 1 h in a hood. Tubes were removed from the heat block and kept at RT for 5 min. Then 800 µl of freshly prepared H_2O / 1.25 % NH_4Molybdate (50 mg/4 ml H_2O) / 1.67 % ascorbic acid (100 mg/6 ml H_2O) in the ratio of 5:2:1 were added. Tubes were heated at 100 °C for 5 min with a marble on each tube to prevent evaporation during heating. Tubes were removed from the block and cooled at RT for 5 min. 100 µl of each sample was then transferred into a 96-well microplate and the absorbance at 820 nm was measured.

Phospho-and Sphingolipid analysis by tandem mass spectrometry

Tandem mass spectrometry for the identification and quantification of phospho- and sphingolipid molecular species was performed using multiple reaction monitoring (MRM) with a TSQ Vantage Triple Stage Quadrupole Mass Spectrometer (Thermo Scientific) equipped with a robotic nanoflow ion source, Nanomate HD (Advion Biosciences, Ithaca, NY). Each individual ion dissociation pathway was optimized with regard to collision energy. Lipid concentrations were calculated relative to the relevant internal standards as described in (27) and then normalized to the total phosphate content of each total lipid extract to adjust for difference in cell size, membrane content and extraction efficiency.

Cellular ceramide glycosylation assay

The cellular ceramide glycosylation assay was performed as described previously (28). Briefly, HeLa cells were treated with siRNA against PIG-F, PIG-O or PIG-U for 70h. Scrambled (SCR) siRNA was used as control. Cells were then switched to 950 μl of 1% BSA DMEM medium containing 10 μM NBD C_6-ceramide for 2h. Cells were then rinsed with ice-cold PBS, scraped and pelleted. Sphingolipids were extracted using the MTBE/methylamine protocol. Samples were resolved on partisil HPTLC plates with fluorescent indicator (Whatman). To distinguish GalCer and GlcCer the HPTLC plates were impregnated with borate as described previously (28). After dipping the plates into a 1% aqueous sodium tetraborate solution the HPTLC plates were activated at 120° C for 30 min. Sphingolipids were resolved with the solvent system of chloroform/MeOH/H_2O (100:30:4). Fluorescent lipids were visualized under UV exposure. NBD C_6-Cer and NBD C6-Cer complexed to BSA were purchased from Invitrogen, NBD C_6-GlcCer and NBD C_6-GalCer were purchased from Matreya. Bands were quantified with the Image J software and values were calculated as percentage of input (NBD C6-Cer).

Determination of GM3 levels

Individual GM3 species were detected by high resolution mass spectrometry on the LTQ Orbitrap XL linear ion trap (Thermo Scientific). Sphingolipid enriched extracts were infused at a low flow rate using the TriVersa NanoMate robotic ESI source (Advion Biosciences) equipped with a standard ESI chip (Advion Biosciences). Samples were analyzed in negative ion mode. Individual GM3 species were identified by their parental mass combined with fragmentation.

Product ions of m/z 290 were obtained from HCD fragmentation of the GM3 precursor ions. These ions correspond to Neu5Ac fragments obtained after cleavage of the glycosidic bond.

Sterol analysis by gas liquid chromatography mass spectrometry.

Extracts were analyzed by GC–MS as described (29). Briefly, samples were injected into a VARIAN CP-3800 gas chromatograph equipped with a Factor Four Capillary Column VF-5ms 15 m × 0.32 mm i.d. DF = 0.10 and analyzed by a Varian 320 MS triple quadrupole with electron energy set to – 70 eV at 250 °C. Samples were applied with the column oven at 45 °C, held for 4 min, then raised to 195 °C (20 °C/min). Sterols were eluted with a linear gradient from 195 to 230 °C (4 °C / min), followed by raising to 320 °C (10 °C / min). Finally, the column temperature was raised to 350 °C (6 °C / min) to elute sterol esters. Cholesterol and cholesterol esters were identified by their retention times (compared to standards) and fragmentation patterns, which were compared to the NIST library.

Statistical analyses

All results are representative of at least 3 independent experiments. Statistical analyses were performed using an unpaired Student's *t*-test. Differences were considered significant for $p < 0.05$ (*), $p < 0.01$ (**) and $p < 0.005$ (***).

Results

The goal of this study was to establish the lipid profile of cells that have a defect in GPI-anchor biosynthesis. CHO GPI-anchor mutants have been very useful in the past to understand the GPI biosynthesis pathway and have allowed cloning of the majority of genes involved in this process (1). We focused on CHO mutants that had either the F21 or the C311 genetic background. The F21 series includes cell lines that are defective in Dol-P-Mannose synthase (DPM3), GPI mannosyltransferase I (PIG-X), ethanolamine phosphate transferase II and III (PIG-F) and GPI lipid remodeling (PGAP2). From the C311 series we analyzed cells defective in ethanolamine phosphate transferase III (PIG-O) and GPI transamidase (PIG-U).

Defects in GPI anchor biosynthesis lead to changes in HexCer levels.

As can be seen in Figure 1 we observed changes in HexCer levels in CHO mutant cells that have a defect in GPI anchor biosynthesis. Since CHO cells do not possess endogenous GalCer (30) the changes in HexCer are due to a difference in their glucosylceramide (GlcCer) levels. In detail, we observed a downregulation of total GlcCer levels in a subset of GPI anchor mutants (DPM3, PIG-X and PIG-F) that generate short truncated GPI anchor intermediates. To our surprise we did not see an effect in GPI anchor mutant PIG-U cells (Fig. 1B). Since PIG-U mutant cells (PA16.1) have no expression of the GPI marker protein CD59 and only 1% remaining DAF expression (Supplemental table 1) this indicates that the observed GlcCer changes are not due to a general absence of GPI anchored proteins (23). Lipid remodeling in the Golgi also did not influence GlcCer levels since we did not observe a change in PGAP2 deficient cells (Fig. 1A), which have normal GPI anchor biosynthesis in the ER but greatly reduced surface expression levels of CD59 and DAF (31) due to rapid secretion (Supplemental table 1). In contrast, the GPI

anchor mutant PIG-O (22), which shows a great reduction but not a complete deficiency in the surface expression of GPI anchored proteins displayed a strong increase in GlcCer-levels (Supplemental table 1, Fig. 1B).

When GlcCers were analyzed in detail we observed an effect concerning the chain length of individual glucosylceramide species. Very long chain GlcCers with a fatty acid chain length of C_{22} and C_{24} were strongly decreased in the GPI anchor mutants DPM3, PIG-X and PIG-F whereas GlcCer species with a fatty acid chain length between C_{10} and C_{20} were mostly unaffected (Fig. 1C). In contrast, PIG-O mutant cells showed a general upregulation of all glucosylceramide species regardless of their chain length (Fig. 1D).

We next focused on the GPI anchor mutants PIG-F and PIG-U, which showed different phenotypes in our lipid analysis. Both GPI-anchor mutants cannot generate GPI-anchored proteins and accumulate free GPI-anchor intermediates that are similar in structure (Fig. 2A). However, PIG-U mutants are deficient in one subunit of the GPI transamidase and accumulate otherwise a functional free GPI anchor. PIG-F mutants on the other hand lack the regulatory subunit of the EtN-P transferases II and III and consequently have no EtN-P on both Man2 and Man3. The EtN-P on Man2 is later recognized and removed by PAGP5, a step which is necessary for efficient incorporation of GPI anchored proteins in to ER exit sites (5). PIG-F and PIG-U mutants belong to different series of CHO mutant cells (F21 and C311 respectively) and carry plasmids, which encode for several GPI anchor biosynthesis enzymes and GPI anchor marker proteins (20, 23). To test if the observed GlcCer changes are due to the defect in GPI anchor biosynthesis or if they are connected to their genetic background, we stably complemented both PIG-F and PIG-U mutant cells with the corresponding wild-type gene. In order to monitor restored GPI anchor biosynthesis we stably coexpressed Venus tagged CD59.

As can be seen in Fig 2B, the GPI anchored protein CD59 localizes to the cell surface in PIG-F complemented cells whereas in the PIG-F deficient control cells, CD59 does not reach the cell surface. We then analyzed the lipid profile from both uncomplemented and complemented cells. As can be seen in Fig. 2C GlcCer levels returned to wild type in the complemented PIG-F cells indicating that the decrease in GlcCer levels was due to their defect in GPI anchor biosynthesis. As expected, we did not observe any changes in PIG-U cells after complementation (Fig. 2C).

We next wanted to see whether the observed sphingolipid changes are CHO cell specific or if they can be reproduced in another mammalian, preferentially human cell line. In addition, we were interested if a transient knockdown of GPI anchor biosynthesis leads to the same sphingolipid changes as a genetic mutation. To test these two parameters, we transiently silenced PIG-L, DPM3, PIG-X, PIG-F, PIG-O, PIG-U and PGAP2 expression in HeLa cells by siRNA. The gene silencing efficiency was confirmed by quantitative RT-PCR (Supplement S1). Hela cells possess ceramide galactosyltransferase activity (32) therefore their HexCer levels might be composed of GlcCer and GalCer species. When analyzed by HPTLC, HeLa cells showed higher levels of GlcCer than GalCer (Supplement S2). As can be seen in Figure 3A we found a decrease in total HexCer levels in PIG-L, DPM3, PIG-X and PIG-F but not in PIG-U or PGAP2 deficient cells. Again very long chain C_{22} and C_{24} HexCer species were strongly affected whereas C_{16} HexCer was only slightly decreased (Fig. 3B). Since HeLa cells have a higher percentage of very long chain C_{22} and C_{24} HexCer species than CHO cells, the decrease in total HexCer was more pronounced. A specific decrease of very long chain HexCer species was also observed for the less abundant sphinganine containing dihydroglycosylceramides (DHHexCer, Supplement S3). Interestingly, PIG-O depleted cells showed again a strong increase in total HexCer levels and a

general upregulation of all HexCer species similar to what had been observed for CHO cells (Fig. 3A, B).

Decrease in HexCer affects downstream glycosphingolipids.

We next analyzed if the observed decrease in GlcCer levels in CHO cells also affects downstream glycosphingolipids such as GM3. The glycosphingolipid profile of CHO cells is rather simple since they only synthesize GlcCer, lactosylceramide and the ganglioside NeuAcα2-3Galβ1-4Glcβ1-1Cer (GM3) (30). CHO cells accumulate high amounts of GM3 since they are unable to synthesize GM2 and other complex gangliosides such as GM1 and GD1a (33). We therefore measured GM3 levels in the GPI anchor mutant CHO cells. When individual GM3 species were analyzed by high-resolution mass spectrometry we found a decrease of the very long chain GM3 species for DPM3, PIG-X and PIG-F but not for PGAP2 deficient cells (Fig. 4A). GM3 levels also did not change in PIG-O and PIG-U deficient cells indicating that the increase in GlcCer levels that was observed in PIG-O deficient cells did not translate into an upregulation of GM3 (Figure 4B). HeLa cells predominantly synthesize Gb3 and have low amounts of GM3 (34), which were below our quantification level.

Ceramide levels are affected by defects in GPI anchor biosynthesis in a cell line dependent manner.

Since ceramides are direct precursors of monoglycosylated ceramides we analyzed if the observed effect on HexCer levels was reflected by a decrease in ceramide. We measured ceramide levels in the same set of GPI anchor mutant CHO cells and found that DPM3, PIG-X and PIG-F cells had reduced ceramide levels whereas no change was observed for PGAP2

deficient cells (Fig 5A). On the individual level very long chain ceramides, in particular C_{24} ceramide were decreased (Fig 5C). In PIG-U and PIG-O mutant cells, ceramide levels were unaffected (Fig. 5B and D). In HeLa cells however, total ceramide levels were not decreased upon knockdown of PIG-L, DPM3, PIG-X or PIG-F (Fig. 5E) and also on the individual level there was no significant change in very long chain ceramides (Fig. 5F). This indicates that the decrease in very long chain ceramides could be cell line specific or might be a compensatory effect of the genetic mutation. In addition, it also raises the possibility that reduced ceramide biosynthesis is not the only cause for the observed decrease in HexCer levels. We next tested if glycosylation of ceramide is affected in the GPI anchor deficient cells. It has been shown that glucosylceramide synthase localizes to the Golgi in HeLa cells (35) but it cannot be fully ruled out that some GlcCer synthase activity might also exist in the ER (36). To test if ceramide glycosylation is affected in the GPI anchor deficient cells we performed an *in vivo* ceramide glycosylation assay (28). As can be seen in Figure 5G NBD-C6 ceramide was efficiently converted into GlcCer in PIG-F, PIG-O and PIG-U depleted cells. There was however no synthesis of GalCer, which shows that ceramide galactosyltransferase activity is very low in HeLa cells (Fig. 5G). Relative to the total amount of input (NBD-C6 Cer) there was an increase in NBD-C6 GlcCer in the PIG-O depleted cells, which indicates more GlcCer synthase activity in PIG-O depleted cells.

Very long chain sphingomyelin levels are partially affected in GPI anchor deficient cells

In contrast to the observed changes in HexCer and ceramide, total sphingomyelin levels were not affected in the same set of GPI anchor mutant CHO cells (Fig. 6A and B). Total sphingomyelin levels also did not change in both the PIG-F and the PIG-U complemented cells (Supplement

S4). However, CHO cells have predominantly C_{16} sphingomyelin, which accounts for 70% of the total sphingomyelin and very long chain sphingomyelins were slightly reduced in CHO mutants that have a decrease in GlcCer levels (Fig. 6C). Total sphingomyelin levels were also not significantly changed in HeLa cells (Fig. 6D) but the detailed analysis showed that defects in GPI anchor biosynthesis have an effect on very long chain sphingomyelins (Fig. 6E). As there is much more sphingomyelin than HexCer in both, CHO and HeLa cells, the absolute amounts of sphingomyelin that are affected could be in fact more than HexCers.

The ceramide transport protein CERT mediates transport of ceramide for sphingomyelin biosynthesis. However, CERT deficiency does not affect total GlcCer levels in CHO cells indicating that there is an alternative ceramide transport pathway for the biosynthesis of GlcCer (18). *In vitro* CERT has a strong preference for the transport of ceramides that are C_{20} or shorter and does not efficiently transport very long chain ceramides (37). We silenced CERT in HeLa cells and observed a decrease in total sphingomyelin as expected (Fig. 7A). HexCer levels did not decrease and even modestly increased which confirms the existence of different ceramide transport pathways (Fig. 7A). As shown in Figure 7B knockdown of CERT affected both C_{16} and C_{24} sphingomyelins indicating that *in vivo* CERT is also required for the efficient transport of very long chain ceramides. This might explain why very long chain sphingomyelins are only partially affected in GPI anchor deficient cells. Individual HexCer levels showed a stronger increase in C_{16} than in C_{22} glycosylceramides (Supplement S5).

Defects in GPI glycan remodeling or GPI anchor trafficking affect HexCer levels.

We had noticed a strong global increase in HexCer levels for PIG-O deficient CHO cells, which was reproduced in HeLa cells during a transient knockdown of PIG-O. In PIG-O deficient cells

ethanolamine phosphate transferase III (PIG-F/GPI7) is active and cells can attach EtN-P onto mannose 2, which is important for glycan remodeling. Interestingly PIG-O mutants are not completely deficient in the surface expression of GPI-anchored proteins and accumulate an intermediate, called KO-2 (Figure 2A), which is competent for protein attachment but has an abnormal glycan structure (38). The glycan structure plays an important role for sorting of GPI anchored proteins into ER exit sites (5, 6) and only glycan remodeled GPI-anchored proteins associate with p24 family proteins (6, 39). We therefore analyzed the lipid profile of cells in which the GPI remodeling enzymes PGAP1, PGAP5 or the p24 family members p23 or p24 were silenced respectively. As can be seen in Figure 8A total HexCer levels increased upon knockdown of PGAP1, PGAP5, p23 and in particular for p24. Individual HexCer levels showed that all HexCer species were affected equally (Fig. 8B). This result is in line with the observed increase of HexCer levels in PIG-O deficient cells and indicates that an abnormal GPI structure or a delay in ER to Golgi transport can lead to an increase in total HexCer levels. We also observed some increase in ceramide levels in particular for PGAP1 but sphingomyelin levels were not changed (Supplement S6, S7). In yeast it has been shown that a defect in GPI anchor remodeling or trafficking results in ER stress and induces the upregulation of the unfolded protein response (UPR) (40-42). We assessed ER stress by measuring transcriptional activation of the UPR. The C/EBP homology protein (CHOP), which is involved in ER stress mediated apoptosis was upregulated in the GPI anchor mutant PIG-O, the remodeling mutants PGAP1 and PGAP5 as well as in p23 and p24 knockdowns but not in PIG-F deficient cells (Figure 8C). The ER chaperone BiP, was upregulated in PIG-O, PGAP5 and p23 depleted cells.

Cholesterol ester levels are reduced in cells that do not synthesize GPI anchored proteins

It has been previously reported that GPI-deficient CHO cells have cholesterol contents similar to wild type CHO cells (43). Using our mass spectrometry approach we measured the amount of free cholesterol and of cholesterol ester in the GPI-anchor deficient CHO and HeLa cells. As can be seen in Figure 9A free cholesterol levels are unchanged between wild type and the GPI anchor mutants. We found, however, that all GPI-anchor mutant cells including PIG-U had lower levels of cholesterol ester than the corresponding wild type cells (Fig. 9A). PIG-O mutant cells, which are not completely deficient in the biosynthesis of GPI anchored proteins, did not show a reduction in cholesterol esters. We then also analyzed the sterol composition of HeLa cells in which PIG-L, DPM3, PIG-F, PIG-O or PIG-U had been silenced respectively. Under these conditions, we observed a similar result: free cholesterol levels were mostly unchanged (Fig. 9B) whereas cholesterol ester levels were strongly reduced in all knockdowns except PIG-O (Fig. 9B). This result suggests that the observed effect on cholesterol ester is due to the inability to synthesize certain GPI anchored proteins and is not caused by a specific GPI anchor intermediate that is generated.

In parallel to the observed changes in glycolipids and sterols we also analyzed the phospholipid content of each GPI anchor mutant by mass spectrometry. We measured the levels of phosphatidylethanolamine (PE), phosphatidylcholine (PC), phosphatidylinositol (PI) and phosphatidylserine (PS). Among those glycerophospholipids we did not observe any major changes except for a mild increase of total PE in the GPI-anchor mutants DPM3, PIG-X and PIG-O (Supplement S8).

Discussion

In this study we show that GPI-anchor biosynthesis mutants that generate incomplete GPI anchor intermediates have a strong decrease in very long chain C_{22} and C_{24} glucosylceramide levels, without greatly affecting long chain C_{16} glucosylceramides. In contrast, GPI transamidase deficient cells (PIG-U) that synthesize complete anchors, but do not attach them to proteins, do not show this effect. This suggests that the GPI anchor, not necessarily attached to proteins, regulates very long chain GlcCer levels. Complementation experiments showed that these changes are specific to the GPI anchor biosynthesis and are not due to the complex genetic background of the GPI anchor mutant cells. siRNA silencing of GPI anchor biosynthesis genes in HeLa cells demonstrated that the observed effects on GlcCers are not restricted to one cell type and that the strategy of siRNA gene downregulation can be used to see changes in lipid profiles in a relatively short time period.

In addition to the decrease in GlcCer we also observed a decrease in very long chain ceramides in the CHO GPI anchor mutants. However this decrease was not observed in HeLa cells following a transient knockdown of the same GPI anchor biosynthesis genes (Fig. 5E). This implies that the decrease in very long chain HexCer is probably not just the consequence of reduced ceramide levels.

Defects in GPI anchor biosynthesis lead to the ER accumulation of GPI anchor intermediates such as GlcNAc-PI and GlcN-acyl-PI as well as the mannose containing GPI intermediates H2-H8 (1). Metabolic labeling with *myo*-[^{3}H]inositol has shown that GPI anchor mutants such as DPM3 and PIG-X accumulate moderate amounts of the early GPI anchor intermediate GlcN-acyl-PI whereas PIG-U mutants show a high ER accumulation of all GPI anchor intermediates (20, 23). In particular, Man-GlcN-(acyl)-PI labels strongly in PIG-U deficient cells cultured with

[^{3}H]mannose, suggesting that GlcN-(acyl)-PI is also elevated in those cells (23). Since GlcCer levels were unaffected in PIG-U deficient cells it is therefore unlikely that the ER accumulation of GPI anchor intermediates is causing an inhibition of certain ceramide synthases or that GlcCer synthase activity would be affected. Another possible reason for reduced ceramide and HexCer levels could be that ER to Golgi transport of ceramide is linked to the transport of GPI anchored proteins and free GPI anchor molecules. If very long chain ceramides are not transported efficiently from the ER and are locally accumulating this could lead to a feedback inhibition of certain ceramide synthases and subsequently to a decrease in HexCers. The degree of feedback inhibition might be different in HeLa versus CHO cells.

In contrast to HexCer, sphingomyelin levels were mostly unaffected in the GPI anchor deficient cells. When analyzed in detail we found that CHO cells have primarily C_{16} sphingomyelin (Fig. 6C). In contrast, HeLa cells have a much higher content of very long chain sphingomyelins (C_{24} sphingomyelin is about 45% of total sphingomyelin) and very long chain sphingomyelin levels were mildly affected in HeLa cells (Fig. 6E). The major fraction of ceramide in mammalian cells is transported to the Golgi in a non-vesicular manner via the ceramide transport protein CERT and mutants in CERT affect mainly sphingomyelin levels, which suggested an alternative mechanism of transport of ceramide destined for GlcCer biosynthesis (18). CERT has a preference for ceramide species with an acyl chain length of C_{20} or less and transports C_{22} and C_{24} ceramide with greatly reduced efficiency *in vitro* (37). However our results show that knockdown of CERT led to a global decrease of all sphingomyelin species and also greatly reduced C_{24} sphingomyelin (Fig. 7B). We therefore conclude that *in vivo* the transport of very long chain ceramides from ER to Golgi for sphingomyelin biosynthesis is regulated by CERT. Interestingly, ER to Golgi trafficking of GPI anchored proteins is normal in CERT deficient cells

(44). Taken together these data support a model in which GPI anchor molecules regulate the transport of very long chain ceramides destined for GlcCer and to some degree also for sphingomyelin biosynthesis.

A common feature among the mutants that show decreased levels of very long chain GlcCer is the accumulation of GPI anchor precursors that have incomplete glycan structures. The GPI anchor mutants PIG-L, DPM3 and PIG-X produce very short truncated GPI anchor intermediates (GlcNAc-PI, GlcN-(acyl)-PI) that are unlikely to leave the ER. The mutant PIG-F however generates a GPI anchor intermediate that possesses an almost complete glycan structure but still has reduced GlcCer levels (Fig. 2A). PIG-F is the regulatory subunit of the GPI EtN-P transferase II (PIG-O/PIG-F) and III (GPI7/PIG-F) (45). Consequently, both EtN-P transferases are not active in PIG-F deficient cells (38) and mutant cells do not attach EtN-P onto mannose 2 or 3 (46). Since EtN-Ps are important for glycan remodeling and ER to Golgi transport we speculate that this abnormal glycan structure makes it impossible for the PIG-F GPI anchor intermediate to exit the ER.

In contrast, PIG-U deficient cells, which make a complete GPI-anchor but lack the enzymatic activity to transfer the free GPI anchor to a protein, have unchanged levels of HexCer. Interestingly, it has been reported that cells generate large pools of free non-proteins linked GPI anchors that exit the ER and are transported to the cell surface (47, 48). While there is no direct evidence that free GPI anchors can be remodeled *in vivo*, it has been shown that free GPI anchors are substrates for remodeling enzymes *in vitro* (5).

In contrast to the mutants PIG-L, DPM3, PIG-X and PIG-F we observed a strong increase in HexCer levels for the GPI anchor mutant PIG-O. This was observed in both, the CHO cell lines as well as HeLa cells under siRNA silencing conditions. PIG-O mutants generate intermediates

with a similar GPI structure as PIG-F. However, the ethanolamine phosphate transferase II, which is a complex of GPI7 and PIG-F is active in PIG-O deficient cells (45). Ethanolamine phosphate transferase II adds EtN-P onto mannose 2, which is important for glycan remodeling by PGAP5 (5). Interestingly PIG-O mutants are not completely deficient in the surface expression of GPI-anchored proteins (38). The surface expression of PIG-O deficient cells is due to a minor GPI anchor intermediate, called KO-2 that is competent for protein attachment. KO-2 has an abnormal glycan structure with most likely four mannoses and EtN-P on Man1 and Man3 (38). An additional EtN-P on mannose 2 might be transitory and is a potential substrate for PGAP5. Because of this abnormal glycan structure we speculate that PIG-O deficient cells might have a defect in sorting of free or protein anchored GPIs into ER exit sites (ERES). The ER exit of GPI anchored proteins is controlled by glycan remodeling and p24 complexes act as cargo receptors for GPI anchor sorting into COPII vesicles (6, 39, 49). In agreement with this model, we observed a global increase in HexCer levels in the remodeling mutants PGAP1, PGAP5 as well as for the p24 family proteins. We did however not detect an increase in GM3 levels in PIG-O depleted cells, which shows that a global increase in HexCer does not necessarily translate into an increase in GM3 and most likely follows a different mechanism. In yeast it has been shown that the unfolded protein response is highly activated in the GPI remodeling mutants (40-42). Here we show that ER stress markers such as CHOP are upregulated in the GPI anchor remodeling and trafficking mutants including PIG-O but not in PIG-F deficient cells (Fig 8C). Recently we have shown that ceramide levels are increased in response to induction of the unfolded protein response (27). Since HexCer synthesis protects against Cer-induced stress in mammalian cells (50, 51) we speculate that the ER stress response might cause the observed increase in HexCer levels in the GPI anchor remodeling mutants.

Finally, we did not observe any sphingolipid changes for the GPI anchor mutant PGAP2, which has normal GPI anchor biosynthesis in the ER but greatly reduced surface expression levels of GPI anchored proteins due to secretion (31). Sorting of GPI-APs into ERES and ER to Golgi trafficking is not affected in the PGAP2 deficient cells.

Concerning the sterol composition of the GPI anchor deficient cells we observed no effect on free cholesterol levels but found a decrease in cholesterol ester (CE) levels in certain GPI anchor deficient cells (Fig. 9). There was however no correlation between the sterol and the HexCer profile since PIG-U deficient cells showed a similar reduction of CE levels as PIG-F deficient cells. In contrast, PGAP2 and PIG-O deficient cells, which synthesize GPI anchored proteins had almost wild type levels of CEs. We therefore speculate that the decrease in cholesterol ester is due to the absence of certain GPI anchored proteins that affect biosynthesis or degradation of cholesterol esters. In addition, uptake of cholesterol from the medium, which contains fetal calf serum might be affected in cells that lack GPI anchored proteins.

GPI-anchored proteins have been postulated to segregate into sphingolipid enriched lipid ordered microdomains (52). In yeast it has been shown that ongoing ceramide synthesis is required for GPI-anchored protein transport from the ER to the Golgi compartment, linking the two processes (10, 11). In mammalian cells however *de novo* sphingolipid biosynthesis is not required to transport mammalian GPI-APs from the ER to the Golgi (15, 53). However, this does not exclude the possibility that also in mammalian cells ER to Golgi transport of ceramide is linked to the transport of GPI anchored proteins. It might be possible that under sphingolipid depleted conditions GPI anchored proteins are trafficked normally but that in the absence of GPI anchored proteins very long chain ceramides are not transported properly.

Taken together we present here a model whereby the levels of very long chain GlcCer are correlated to the biosynthesis of GPI anchor molecules. We propose that very long chain GlcCer levels and to some extent also very long chain sphingomyelin levels are linked to GPI biosynthesis to ensure that proportional amounts of each lipid class are synthesized and transported.

Acknowledgments

We are grateful to Morihisa Fujita and Yusuke Maeda (Osaka University, Japan) for critical reading, plasmids and cell lines. We thank Adrien Schmid (EPFL, Switzerland), Nicolas Guex (University of Lausanne, Switzerland) and Isabelle Riezman (University of Geneva, Switzerland) for mass spectrometry support and Reika Watanabe (University of Geneva, Switzerland) for plasmids and discussion.

This project was supported by the Swiss National Science Foundation (HR) and the Swiss SystemsX.ch initiative, evaluated by the Swiss National Science Foundation.

References

1. Maeda, Y., H. Ashida, and T. Kinoshita. 2006. CHO glycosylation mutants: GPI anchor. *Methods Enzymol* **416**: 182-205.
2. Butikofer, P., T. Malherbe, M. Boschung, and I. Roditi. 2001. GPI-anchored proteins: now you see 'em, now you don't. *FASEB J* **15**: 545-548.
3. Kanzawa, N., Y. Maeda, H. Ogiso, Y. Murakami, R. Taguchi, and T. Kinoshita. 2009. Peroxisome dependency of alkyl-containing GPI-anchor biosynthesis in the endoplasmic reticulum. *Proc Natl Acad Sci U S A* **106**: 17711-17716.
4. Tanaka, S., Y. Maeda, Y. Tashima, and T. Kinoshita. 2004. Inositol deacylation of glycosylphosphatidylinositol-anchored proteins is mediated by mammalian PGAP1 and yeast Bst1p. *J Biol Chem* **279**: 14256-14263.
5. Fujita, M., Y. Maeda, M. Ra, Y. Yamaguchi, R. Taguchi, and T. Kinoshita. 2009. GPI glycan remodeling by PGAP5 regulates transport of GPI-anchored proteins from the ER to the Golgi. *Cell* **139**: 352-365.
6. Fujita, M., R. Watanabe, N. Jaensch, M. Romanova-Michaelides, T. Satoh, M. Kato, H. Riezman, Y. Yamaguchi, Y. Maeda, and T. Kinoshita. 2011. Sorting of GPI-anchored proteins into ER exit sites by p24 proteins is dependent on remodeled GPI. *The Journal of cell biology* **194**: 61-75.
7. Maeda, Y., Y. Tashima, T. Houjou, M. Fujita, T. Yoko-o, Y. Jigami, R. Taguchi, and T. Kinoshita. 2007. Fatty acid remodeling of GPI-anchored proteins is required for their raft association. *Mol Biol Cell* **18**: 1497-1506.
8. Schroeder, R. J., S. N. Ahmed, Y. Zhu, E. London, and D. A. Brown. 1998. Cholesterol and sphingolipid enhance the Triton X-100 insolubility of glycosylphosphatidylinositol-anchored proteins by

promoting the formation of detergent-insoluble ordered membrane domains. *J Biol Chem* **273**: 1150-1157.
9. Hanada, K., M. Nishijima, Y. Akamatsu, and R. E. Pagano. 1995. Both sphingolipids and cholesterol participate in the detergent insolubility of alkaline phosphatase, a glycosylphosphatidylinositol-anchored protein, in mammalian membranes. *J Biol Chem* **270**: 6254-6260.
10. Horvath, A., C. Sutterlin, U. Manning-Krieg, N. R. Movva, and H. Riezman. 1994. Ceramide synthesis enhances transport of GPI-anchored proteins to the Golgi apparatus in yeast. *EMBO J* **13**: 3687-3695.
11. Watanabe, R., K. Funato, K. Venkataraman, A. H. Futerman, and H. Riezman. 2002. Sphingolipids are required for the stable membrane association of glycosylphosphatidylinositol-anchored proteins in yeast. *J Biol Chem* **277**: 49538-49544.
12. Okamoto, M., T. Yoko-o, M. Umemura, K. Nakayama, and Y. Jigami. 2006. Glycosylphosphatidylinositol-anchored proteins are required for the transport of detergent-resistant microdomain-associated membrane proteins Tat2p and Fur4p. *The Journal of biological chemistry* **281**: 4013-4023.
13. Mays, R. W., K. A. Siemers, B. A. Fritz, A. W. Lowe, G. van Meer, and W. J. Nelson. 1995. Hierarchy of mechanisms involved in generating Na/K-ATPase polarity in MDCK epithelial cells. *J Cell Biol* **130**: 1105-1115.
14. Ledesma, M. D., K. Simons, and C. G. Dotti. 1998. Neuronal polarity: essential role of protein-lipid complexes in axonal sorting. *Proc Natl Acad Sci U S A* **95**: 3966-3971.
15. Rivier, A. S., G. A. Castillon, L. Michon, M. Fukasawa, M. Romanova-Michaelides, N. Jaensch, K. Hanada, and R. Watanabe. 2010. Exit of GPI-anchored proteins from the ER differs in yeast and mammalian cells. *Traffic* **11**: 1017-1033.
16. Yamaji, T., K. Kumagai, N. Tomishige, and K. Hanada. 2008. Two sphingolipid transfer proteins, CERT and FAPP2: their roles in sphingolipid metabolism. *IUBMB Life* **60**: 511-518.
17. Hanada, K., T. Hara, M. Fukasawa, A. Yamaji, M. Umeda, and M. Nishijima. 1998. Mammalian cell mutants resistant to a sphingomyelin-directed cytolysin. Genetic and biochemical evidence for complex formation of the LCB1 protein with the LCB2 protein for serine palmitoyltransferase. *J Biol Chem* **273**: 33787-33794.
18. Hanada, K., K. Kumagai, S. Yasuda, Y. Miura, M. Kawano, M. Fukasawa, and M. Nishijima. 2003. Molecular machinery for non-vesicular trafficking of ceramide. *Nature* **426**: 803-809.
19. Funato, K., and H. Riezman. 2001. Vesicular and nonvesicular transport of ceramide from ER to the Golgi apparatus in yeast. *J Cell Biol* **155**: 949-959.
20. Ashida, H., Y. Hong, Y. Murakami, N. Shishioh, N. Sugimoto, Y. U. Kim, Y. Maeda, and T. Kinoshita. 2005. Mammalian PIG-X and yeast Pbn1p are the essential components of glycosylphosphatidylinositol-mannosyltransferase I. *Mol Biol Cell* **16**: 1439-1448.
21. Hong, Y., J. Y. Kang, Y. U. Kim, D. J. Shin, H. E. Choy, Y. Maeda, and T. Kinoshita. 2005. New mutant Chinese hamster ovary cell representing an unknown gene for attachment of glycosylphosphatidylinositol to proteins. *Biochem Biophys Res Commun* **335**: 1060-1069.
22. Hong, Y., K. Ohishi, N. Inoue, J. Y. Kang, H. Shime, Y. Horiguchi, F. G. van der Goot, N. Sugimoto, and T. Kinoshita. 2002. Requirement of N-glycan on GPI-anchored proteins for efficient binding of aerolysin but not Clostridium septicum alpha-toxin. *EMBO J* **21**: 5047-5056.
23. Hong, Y., K. Ohishi, J. Y. Kang, S. Tanaka, N. Inoue, J. Nishimura, Y. Maeda, and T. Kinoshita. 2003. Human PIG-U and yeast Cdc91p are the fifth subunit of GPI transamidase that attaches GPI-anchors to proteins. *Molecular biology of the cell* **14**: 1780-1789.
24. Oslowski, C. M., and F. Urano. 2011. Measuring ER stress and the unfolded protein response using mammalian tissue culture system. *Methods in enzymology* **490**: 71-92.

25. Matyash, V., G. Liebisch, T. V. Kurzchalia, A. Shevchenko, and D. Schwudke. 2008. Lipid extraction by methyl-tert-butyl ether for high-throughput lipidomics. *J Lipid Res* **49**: 1137-1146.
26. Clarke, N. G., and R. M. Dawson. 1981. Alkaline O leads to N-transacylation. A new method for the quantitative deacylation of phospholipids. *Biochem J* **195**: 301-306.
27. Epstein, S., C. L. Kirkpatrick, G. A. Castillon, M. Muniz, I. Riezman, F. P. David, C. B. Wollheim, and H. Riezman. 2011. Activation of the unfolded protein response pathway causes ceramide accumulation in yeast and INS-1E insulinoma cells. *Journal of lipid research*.
28. Gupta, V., G. A. Patwardhan, Q. J. Zhang, M. C. Cabot, S. M. Jazwinski, and Y. Y. Liu. 2010. Direct quantitative determination of ceramide glycosylation in vivo: a new approach to evaluate cellular enzyme activity of glucosylceramide synthase. *Journal of lipid research* **51**: 866-874.
29. Guan, X. L., I. Riezman, M. R. Wenk, and H. Riezman. 2010. Yeast lipid analysis and quantification by mass spectrometry. *Methods Enzymol* **470**: 369-391.
30. van der Bijl, P., G. J. Strous, M. Lopes-Cardozo, J. Thomas-Oates, and G. van Meer. 1996. Synthesis of non-hydroxy-galactosylceramides and galactosyldiglycerides by hydroxy-ceramide galactosyltransferase. *The Biochemical journal* **317 (Pt 2)**: 589-597.
31. Tashima, Y., R. Taguchi, C. Murata, H. Ashida, T. Kinoshita, and Y. Maeda. 2006. PGAP2 is essential for correct processing and stable expression of GPI-anchored proteins. *Mol Biol Cell* **17**: 1410-1420.
32. Yamaji, T., K. Nishikawa, and K. Hanada. 2010. Transmembrane BAX inhibitor motif containing (TMBIM) family proteins perturbs a trans-Golgi network enzyme, Gb3 synthase, and reduces Gb3 biosynthesis. *The Journal of biological chemistry* **285**: 35505-35518.
33. Rosales Fritz, V. M., J. L. Daniotti, and H. J. Maccioni. 1997. Chinese hamster ovary cells lacking GM1 and GD1a synthesize gangliosides upon transfection with human GM2 synthase. *Biochimica et biophysica acta* **1354**: 153-158.
34. Okuda, T., and K. Nakayama. 2008. Identification and characterization of the human Gb3/CD77 synthase gene promoter. *Glycobiology* **18**: 1028-1035.
35. Halter, D., S. Neumann, S. M. van Dijk, J. Wolthoorn, A. M. de Maziere, O. V. Vieira, P. Mattjus, J. Klumperman, G. van Meer, and H. Sprong. 2007. Pre- and post-Golgi translocation of glucosylceramide in glycosphingolipid synthesis. *The Journal of cell biology* **179**: 101-115.
36. Kohyama-Koganeya, A., T. Sasamura, E. Oshima, E. Suzuki, S. Nishihara, R. Ueda, and Y. Hirabayashi. 2004. Drosophila glucosylceramide synthase: a negative regulator of cell death mediated by proapoptotic factors. *The Journal of biological chemistry* **279**: 35995-36002.
37. Kumagai, K., S. Yasuda, K. Okemoto, M. Nishijima, S. Kobayashi, and K. Hanada. 2005. CERT mediates intermembrane transfer of various molecular species of ceramides. *J Biol Chem* **280**: 6488-6495.
38. Hong, Y., Y. Maeda, R. Watanabe, N. Inoue, K. Ohishi, and T. Kinoshita. 2000. Requirement of PIG-F and PIG-O for transferring phosphoethanolamine to the third mannose in glycosylphosphatidylinositol. *J Biol Chem* **275**: 20911-20919.
39. Takida, S., Y. Maeda, and T. Kinoshita. 2008. Mammalian GPI-anchored proteins require p24 proteins for their efficient transport from the ER to the plasma membrane. *The Biochemical journal* **409**: 555-562.
40. Castillon, G. A., A. Aguilera-Romero, J. Manzano-Lopez, S. Epstein, K. Kajiwara, K. Funato, R. Watanabe, H. Riezman, and M. Muniz. 2011. The yeast p24 complex regulates GPI-anchored protein transport and quality control by monitoring anchor remodeling. *Molecular biology of the cell* **22**: 2924-2936.
41. Jonikas, M. C., S. R. Collins, V. Denic, E. Oh, E. M. Quan, V. Schmid, J. Weibezahn, B. Schwappach, P. Walter, J. S. Weissman, and M. Schuldiner. 2009. Comprehensive characterization of genes required for protein folding in the endoplasmic reticulum. *Science* **323**: 1693-1697.

42. Promlek, T., Y. Ishiwata-Kimata, M. Shido, M. Sakuramoto, K. Kohno, and Y. Kimata. 2011. Membrane aberrancy and unfolded proteins activate the endoplasmic reticulum stress sensor Ire1 in different ways. *Molecular biology of the cell* **22**: 3520-3532.
43. Abrami, L., M. Fivaz, T. Kobayashi, T. Kinoshita, R. G. Parton, and F. G. van der Goot. 2001. Cross-talk between caveolae and glycosylphosphatidylinositol-rich domains. *J Biol Chem* **276**: 30729-30736.
44. Fukasawa, M., M. Nishijima, and K. Hanada. 1999. Genetic evidence for ATP-dependent endoplasmic reticulum-to-Golgi apparatus trafficking of ceramide for sphingomyelin synthesis in Chinese hamster ovary cells. *The Journal of cell biology* **144**: 673-685.
45. Shishioh, N., Y. Hong, K. Ohishi, H. Ashida, Y. Maeda, and T. Kinoshita. 2005. GPI7 is the second partner of PIG-F and involved in modification of glycosylphosphatidylinositol. *The Journal of biological chemistry* **280**: 9728-9734.
46. Puoti, A., and A. Conzelmann. 1993. Characterization of abnormal free glycophosphatidylinositols accumulating in mutant lymphoma cells of classes B, E, F, and H. *The Journal of biological chemistry* **268**: 7215-7224.
47. Baumann, N. A., J. Vidugiriene, C. E. Machamer, and A. K. Menon. 2000. Cell surface display and intracellular trafficking of free glycosylphosphatidylinositols in mammalian cells. *J Biol Chem* **275**: 7378-7389.
48. Singh, N., L. N. Liang, M. L. Tykocinski, and A. M. Tartakoff. 1996. A novel class of cell surface glycolipids of mammalian cells. Free glycosyl phosphatidylinositols. *The Journal of biological chemistry* **271**: 12879-12884.
49. Bonnon, C., M. W. Wendeler, J. P. Paccaud, and H. P. Hauri. 2010. Selective export of human GPI-anchored proteins from the endoplasmic reticulum. *J Cell Sci* **123**: 1705-1715.
50. Niimura, Y., T. Moue, N. Takahashi, and K. Nagai. 2010. Modification of sphingoglycolipids and sulfolipids in kidney cell lines under heat stress: activation of monohexosylceramide synthesis as a ceramide scavenger. *Glycobiology* **20**: 710-717.
51. Uchida, Y., S. Murata, M. Schmuth, M. J. Behne, J. D. Lee, S. Ichikawa, P. M. Elias, Y. Hirabayashi, and W. M. Holleran. 2002. Glucosylceramide synthesis and synthase expression protect against ceramide-induced stress. *Journal of lipid research* **43**: 1293-1302.
52. Fujita, M., M. Umemura, T. Yoko-o, and Y. Jigami. 2006. PER1 is required for GPI-phospholipase A2 activity and involved in lipid remodeling of GPI-anchored proteins. *Mol Biol Cell* **17**: 5253-5264.
53. Sutterwala, S. S., C. H. Creswell, S. Sanyal, A. K. Menon, and J. D. Bangs. 2007. De novo sphingolipid synthesis is essential for viability, but not for transport of glycosylphosphatidylinositol-anchored proteins, in African trypanosomes. *Eukaryot Cell* **6**: 454-464.

Figure legends

Figure 1 Glucosylceramide profile of GPI-anchor deficient CHO cells.

(A) Total GlcCer levels in F21 (wild type) and GPI-anchor mutants DPM3, PIG-X, PIG-F and PGAP2. (B) Total GlcCer levels in C311 (wild type) and GPI-anchor mutant cell lines PIG-O and PIG-U. (C) Individual GlcCer profile of GPI anchor mutants from the F21 series and (D) mutants from the C311 series.

Figure 2 Complementation of the GPI anchor mutants PIG-F and PIG-U

(A) Biosynthetic pathway of mammalian GPI-APs. (1) GPI-*N*-acetylglucosamine transferase, (2) GlcNAc-PI de-*N*-acetylase (PIG-L), (3) Flippase, (4) Inositol acyltransferase, (5) PI remodeling enzyme, (6) GPI-MT I (PIG-M/PIG-X), (7) GPI-MT II, (8) EtN-P transferase I, (9) GPI-MT III, (10) EtN-P transferase III (PIG-O/PIG-F), (11) EtN-P transferase II (PIG-G/PIG-F), (12) GPI transamidase (PIG-K, GAA1, PIG-S, PIG-T, PIG-U), (13) Inositol deacylase (PGAP1), (14) EtN-P Phosphoesterase (PGAP5). ● decreased levels of HexCer, ● unchanged levels of HexCer, ● elevated levels of HexCer. Red arrows indicate a reduction in cholesterol ester levels. (B) Left panel: PIG-F mutant CHO cells (CHO PIG-F -/-) stably expressing Venus-CD59. Right panel: PIG-F mutant CHO cells (CHO PIG-F -/-) stably expressing Venus-CD59 and human PIG-F. Bar = 10 μm. (C) Relative GlcCer levels in the GPI-anchor mutants PIG-F and PIG-U and in the complemented PIG-Fc and PIG-Uc cells. GlcCer levels were calculated as percentage of PIG-Fc and PIG-Uc respectively. *$p < 0.05$ uncomplemented versus complemented cells.

Figure 3 HexCer profile of GPI anchor deficient HeLa cells.

(A) Total HexCer levels of HeLa cells treated with siRNA against PIG-L, DPM3, PIG-X, PIG-F, PIG-O, PIG-U or PGAP2, respectively. Scrambled (SCR) siRNA was used as control. Cells were harvested 72 h after transfection. (B) Individual HexCer levels of the GPI anchor deficient HeLa cells. *$p < 0.05$ and **$p < 0.01$ SCR versus siRNA treated cells.

Figure 4 GM3 levels of GPI-anchor mutant CHO cells

(A) Individual GM3 profile of wild type (F21) and GPI-anchor mutant cell lines DPM3, PIG-X, PIG-F and PGAP2. (B) Individual GM3 profile of wild type (C311) and GPI-anchor mutant PIG-O and PIG-U cells. *$p < 0.05$ wild type versus GPI anchor mutant.

Figure 5 Ceramide profile of GPI anchor deficient cells

(A) Total ceramide (Cer) levels in F21 wild type and GPI-anchor mutants DPM3, PIG-X, PIG-F and PGAP2. (B) Total Cer levels in C311 wild type and GPI-anchor mutant cell lines PIG-O and PIG-U. (C) Individual Cer profile of GPI anchor mutants from the F21 series and (D) mutants from the C311 series. (E) Total Cer and (F) individual Cer levels of HeLa cells treated with siRNA against PIG-L, DPM3, PIG-X, PIG-F, PIG-O, PIG-U or PGAP2, respectively. Scrambled (SCR) siRNA was used as control. ***$p < 0.005$ wild type versus GPI anchor mutant. (G) Ceramide glycosylation assay: HeLa cells were treated with siRNA against PIG-F, PIG-O and PIG-U respectively. After 70h, cells were incubated with NBD C6-Cer for 2h after which sphingolipids were extracted. Lipid extracts were resolved on borate impregnated HPTLC plates and visualized under UV exposure. Standards were NBD C6-Cer, NBD C6-GlcCer and NBD C6

GalCer. Bands were quantified with Image J software and values were calculated as percentage of input (NBD C6-Cer).

Figure 6 Sphingomyelin levels do not change in the GPI deficient cells

(A) Total sphingomyelin (SM) levels of F21 wild type and GPI-anchor mutant cell lines DPM3, PIG-X, PIG-F and PGAP2. (B) Total SM levels of C311 wild type and GPI-anchor mutant cell lines PIG-O and PIG-U. (C) Individual SM levels in the F21 series of GPI anchor mutants. (D) Total SM levels of Hela cells treated with siRNA gainst PIG-L, DPM3, PIG-X, PIG-F, PIG-O, PIG-U and PGAP2. Scrambled (SCR) siRNA was used as control. (E) Individual SM profile of GPI anchor deficient HeLa cells.

Figure 7 CERT knockdown does not lead to a decrease in HexCer levels.

(A) Total sphingomyelin and HexCer levels of Hela cells treated with siRNA against the ceramide transport protein CERT. Scrambled (SCR) siRNA was used as control. (B) Individual sphingomyelin profile of HeLa cells treated with siRNA against CERT. **$p < 0.01$ SCR versus siRNA knockdown.

Figure 8 HexCer levels are affected by GPI glycan remodeling and involve the p24 family members

(A) Total HexCer levels of Hela cells treated with siRNA against PGAP1, PGAP5, p23 or p24, respectively. Scrambled (SCR) siRNA was used as control. (B) Detailed HexCer profile of the corresponding cells. (C) Real time RT-PCR analysis of genes involved in UPR induction. HeLa

cells were treated with siRNA against PIG-F, PIG-O, PGAP1, PGAP5, p23 and p24. SCR was used as control. Cells were harvested 72h after transfection and total RNA was isolated. Relative levels of CHOP and BiP were assessed by qRT-PCR.

Figure 9 Sterol levels in the GPI anchor deficient cells

(A) Free cholesterol and cholesterol ester levels in in the GPI-anchor deficient CHO cell lines DPM3, PIG-X, PIG-F, PIG-O and PIG-U. Values were calculated as percentage of wild type (F21 or C311 respectively). (B) Free cholesterol and cholesterol ester levels in HeLa cells after a transient knockdown of the GPI anchor biosynthesis genes PIG-L, DPM3, PIG-F PIG-O and PIG-U respectively. Scrambled (SCR) siRNA was used as control.

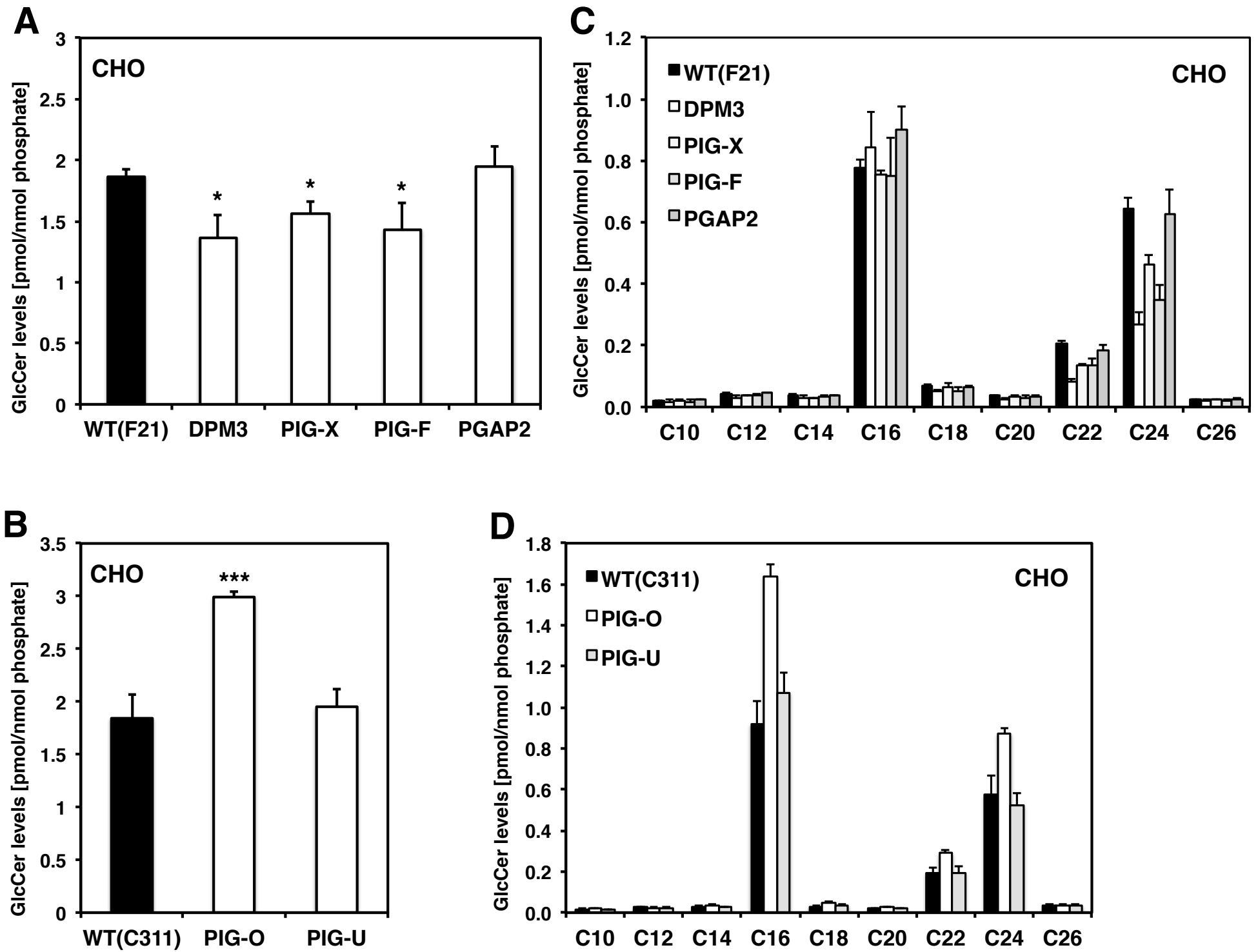
A
CHO
GlcCer levels [pmol/nmol phosphate]
3
2.5
2
1.5
1
0.5
0
*
*
*
WT(F21)
DPM3
PIG-X
PIG-F
PGAP2
C
CHO
WT(F21)
DPM3
PIG-X
PIG-F
PGAP2
GlcCer levels [pmol/nmol phosphate]
1.2
1.0
0.8
0.6
0.4
0.2
0.0
C10
C12
C14
C16
C18
C20
C22
C24
C26
B
CHO
***
GlcCer levels [pmol/nmol phosphate]
3.5
3
2.5
2
1.5
1
0.5
0
WT(C311)
PIG-O
PIG-U
D
CHO
WT(C311)
PIG-O
PIG-U
GlcCer levels [pmol/nmol phosphate]
1.8
1.6
1.4
1.2
1.0
0.8
0.6
0.4
0.2
0.0
C10
C12
C14
C16
C18
C20
C22
C24
C26

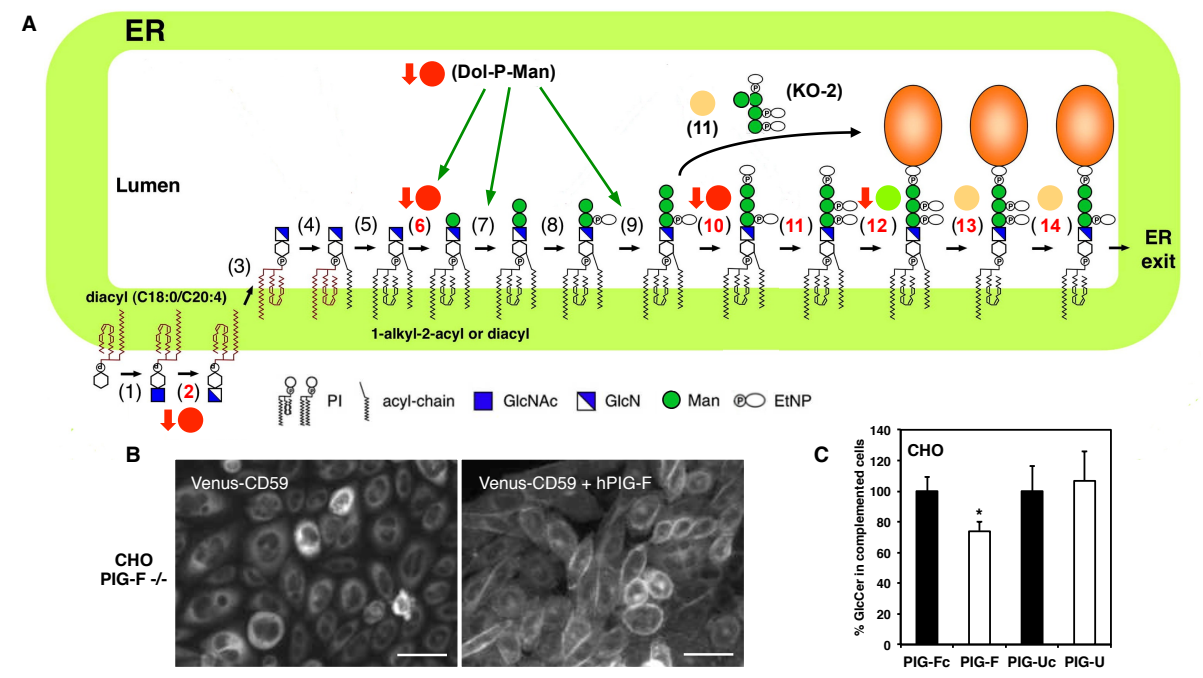
A
ER
Lumen
(Dol-P-Man)
(KO-2)
(11)
(3)
(4)
(5)
(6)
(7)
(8)
(9)
(10)
(11)
(12)
(13)
(14)
ER exit
diacyl (C18:0/C20:4)
1-alkyl-2-acyl or diacyl
(1)
(2)
PI
acyl-chain
GlcNAc
GlcN
Man
EtNP
B
CHO
PIG-F -/-
Venus-CD59
Venus-CD59 + hPIG-F
C
CHO
% GlcCer in complemented cells
0
20
40
60
80
100
120
140
*
PIG-Fc
PIG-F
PIG-Uc
PIG-U

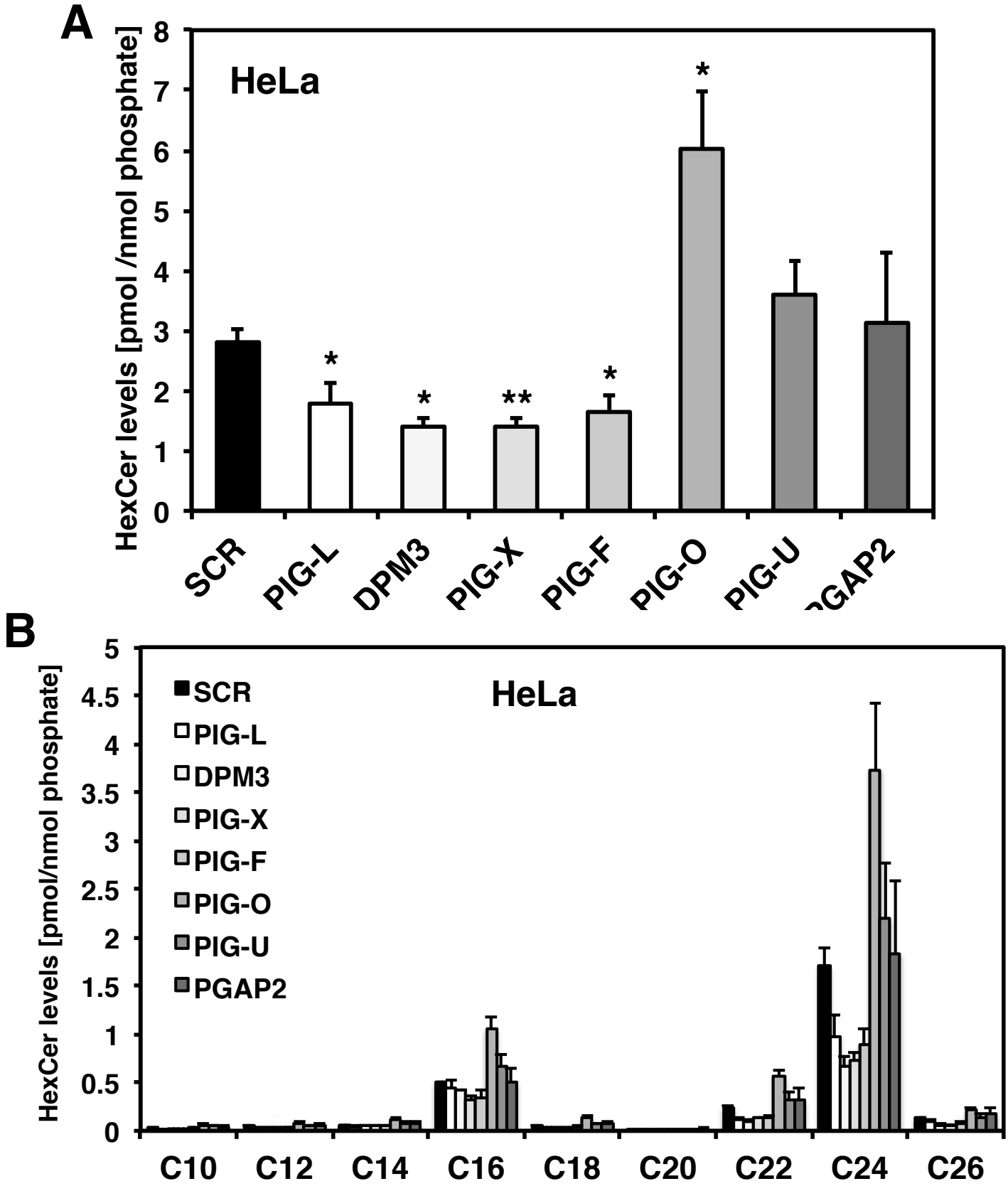
A
HeLa
HexCer levels [pmol /nmol phosphate]
0
1
2
3
4
5
6
7
8
*
*
*
**
*
SCR
PIG-L
DPM3
PIG-X
PIG-F
PIG-O
PIG-U
PGAP2
B
HeLa
HexCer levels [pmol/nmol phosphate]
SCR
PIG-L
DPM3
PIG-X
PIG-F
PIG-O
PIG-U
PGAP2
0
0.5
1
1.5
2
2.5
3
3.5
4
4.5
5
C10
C12
C14
C16
C18
C20
C22
C24
C26

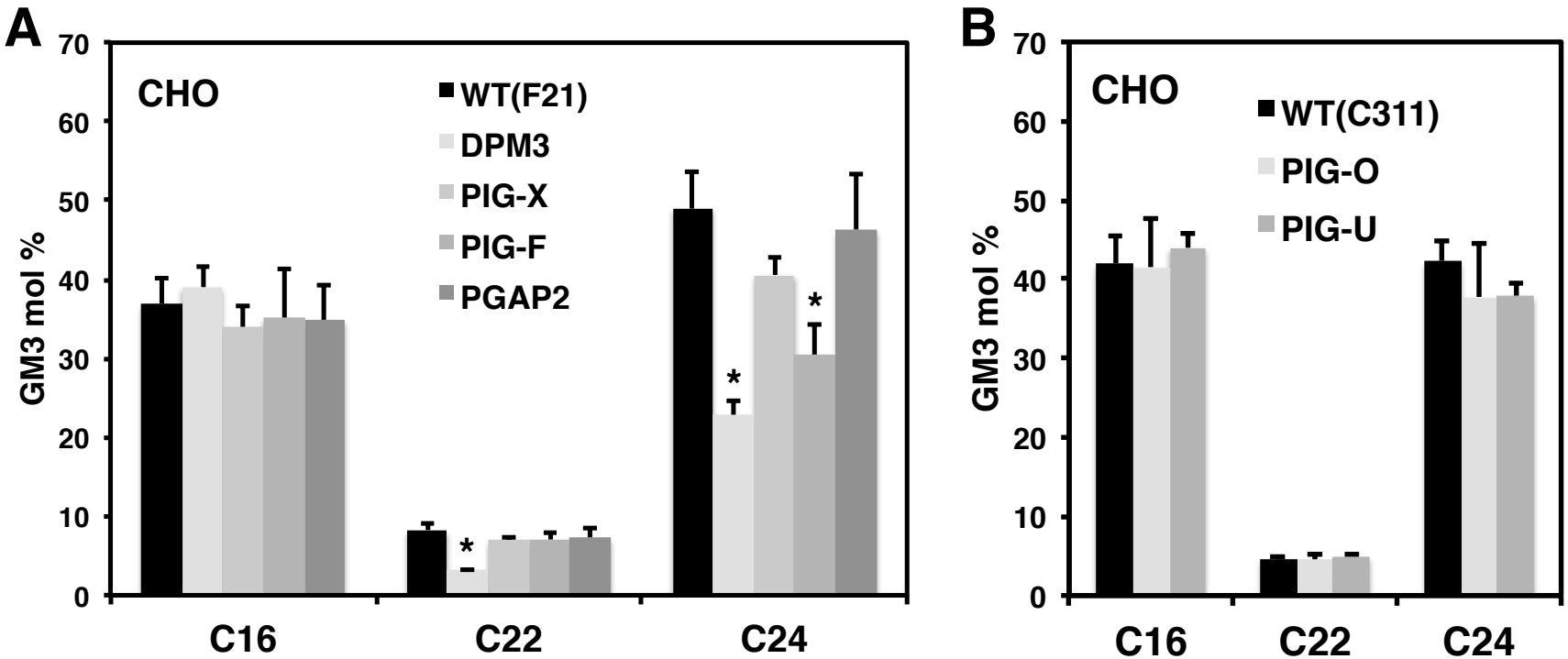
A
CHO
WT(F21)
DPM3
PIG-X
PIG-F
PGAP2
GM3 mol %
70
60
50
40
30
20
10
0
C16
C22
C24
*
*
*
B
CHO
WT(C311)
PIG-O
PIG-U
GM3 mol %
70
60
50
40
30
20
10
0
C16
C22
C24

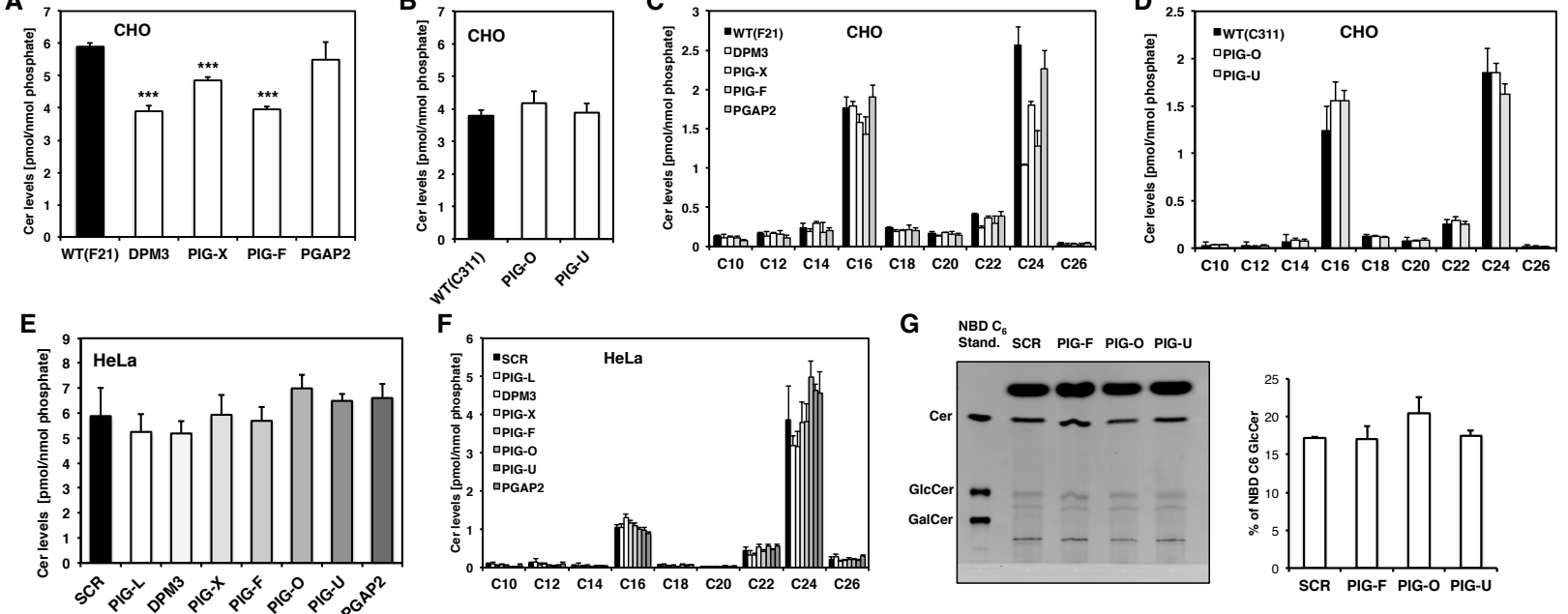
A
CHO
Cer levels [pmol/nmol phosphate]
***
***
***
WT(F21)
DPM3
PIG-X
PIG-F
PGAP2
B
CHO
Cer levels [pmol/nmol phosphate]
WT(C311)
PIG-O
PIG-U
C
CHO
WT(F21)
DPM3
PIG-X
PIG-F
PGAP2
Cer levels [pmol/nmol phosphate]
C10
C12
C14
C16
C18
C20
C22
C24
C26
D
CHO
WT(C311)
PIG-O
PIG-U
Cer levels [pmol/nmol phosphate]
C10
C12
C14
C16
C18
C20
C22
C24
C26
E
HeLa
Cer levels [pmol/nmol phosphate]
SCR
PIG-L
DPM3
PIG-X
PIG-F
PIG-O
PIG-U
PGAP2
F
HeLa
SCR
PIG-L
DPM3
PIG-X
PIG-F
PIG-O
PIG-U
PGAP2
Cer levels [pmol/nmol phosphate]
C10
C12
C14
C16
C18
C20
C22
C24
C26
G
NBD C6
Stand.
SCR
PIG-F
PIG-O
PIG-U
Cer
GlcCer
GalCer
% of NBD C6 GlcCer
SCR
PIG-F
PIG-O
PIG-U

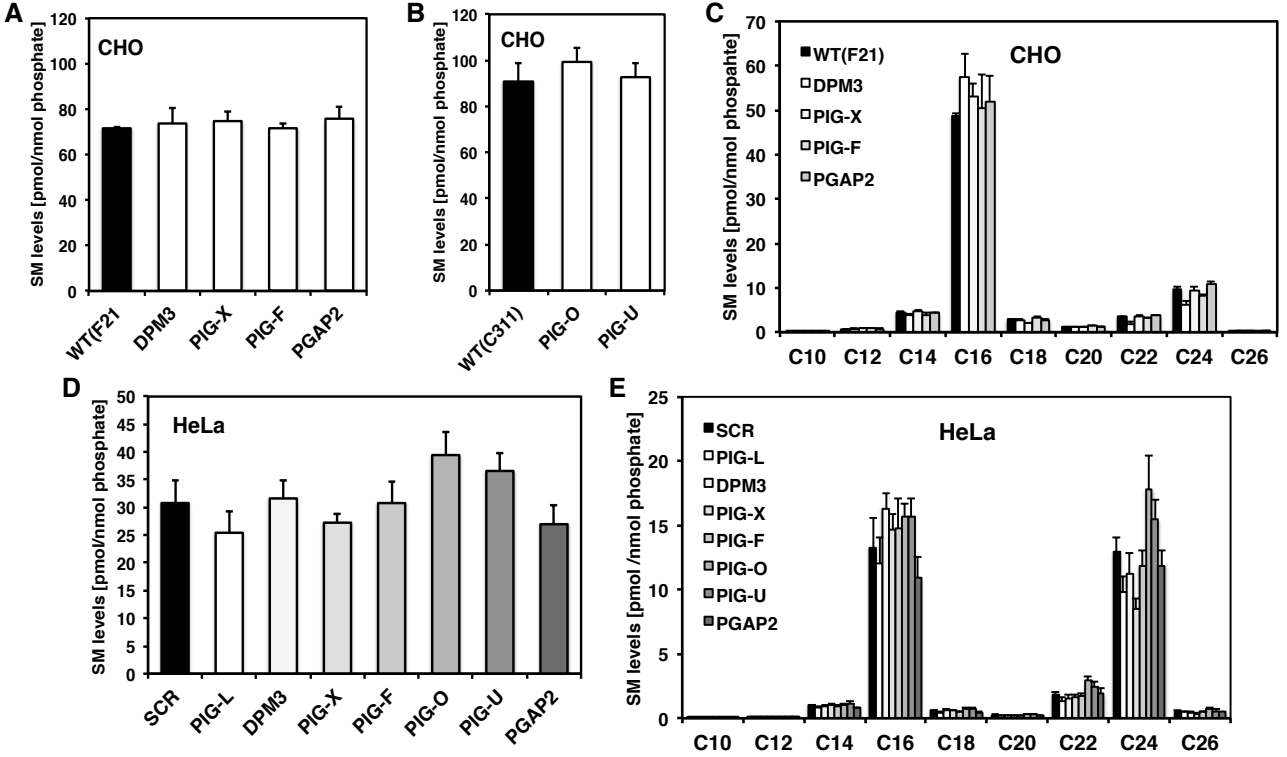
A
CHO
SM levels [pmol/nmol phosphate]
WT(F21
DPM3
PIG-X
PIG-F
PGAP2
B
CHO
SM levels [pmol/nmol phosphate]
WT(C311)
PIG-O
PIG-U
C
CHO
WT(F21)
DPM3
PIG-X
PIG-F
PGAP2
SM levels [pmol/nmol phospahte]
C10 C12 C14 C16 C18 C20 C22 C24 C26
D
HeLa
SM levels [pmol/nmol phosphate]
SCR
PIG-L
DPM3
PIG-X
PIG-F
PIG-O
PIG-U
PGAP2
E
HeLa
SCR
PIG-L
DPM3
PIG-X
PIG-F
PIG-O
PIG-U
PGAP2
SM levels [pmol /nmol phosphate]
C10 C12 C14 C16 C18 C20 C22 C24 C26

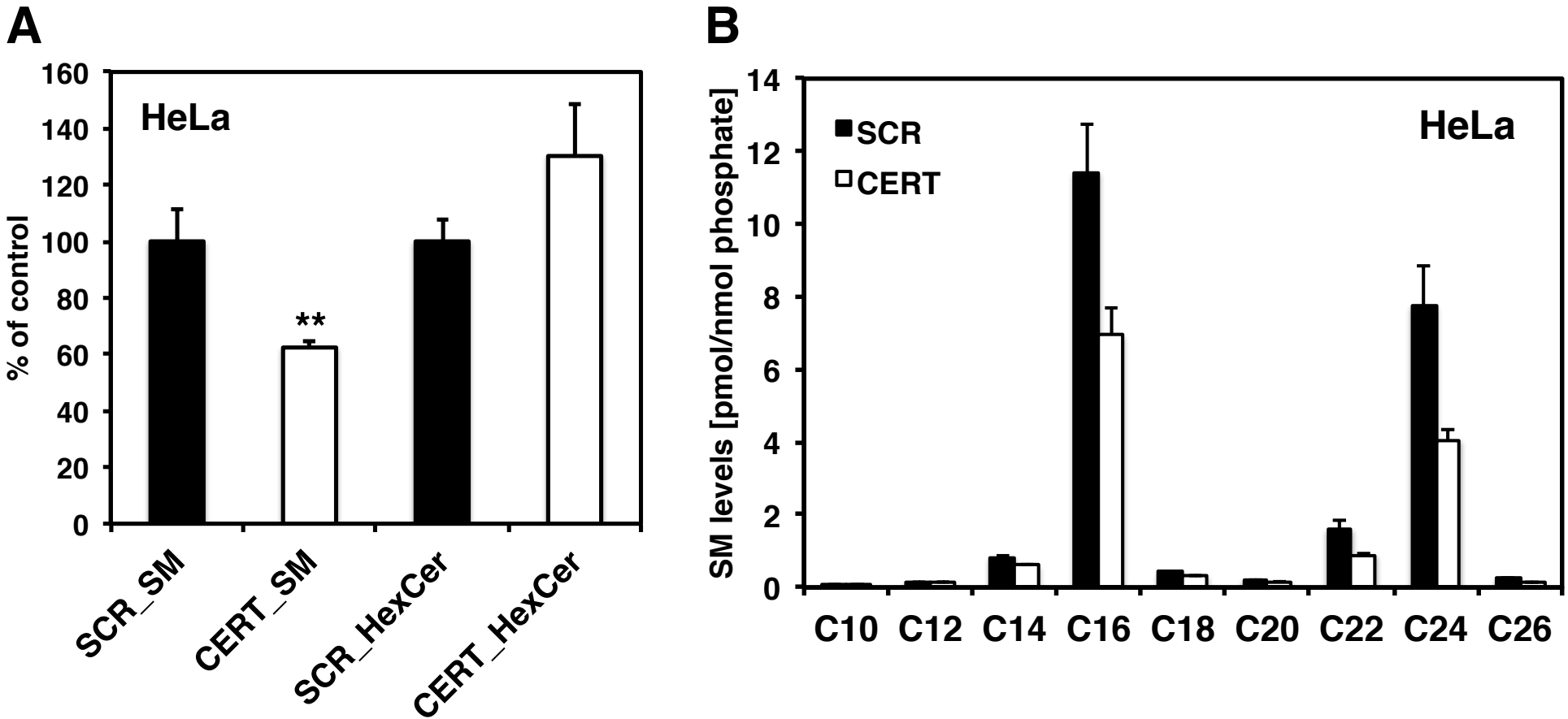
A
HeLa
% of control
160
140
120
100
80
60
40
20
0
**
SCR_SM
CERT_SM
SCR_HexCer
CERT_HexCer
B
HeLa
SCR
CERT
SM levels [pmol/nmol phosphate]
14
12
10
8
6
4
2
0
C10
C12
C14
C16
C18
C20
C22
C24
C26

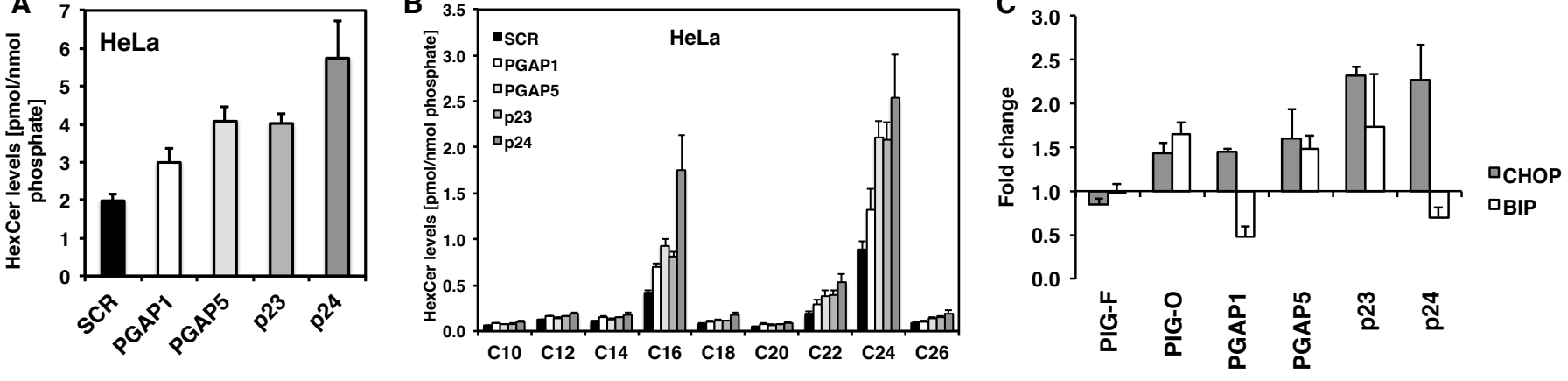
A
HeLa
HexCer levels [pmol/nmol phosphate]
SCR
PGAP1
PGAP5
p23
p24
B
HeLa
SCR
PGAP1
PGAP5
p23
p24
HexCer levels [pmol/nmol phosphate]
C10
C12
C14
C16
C18
C20
C22
C24
C26
C
Fold change
CHOP
BIP
PIG-F
PIG-O
PGAP1
PGAP5
p23
p24

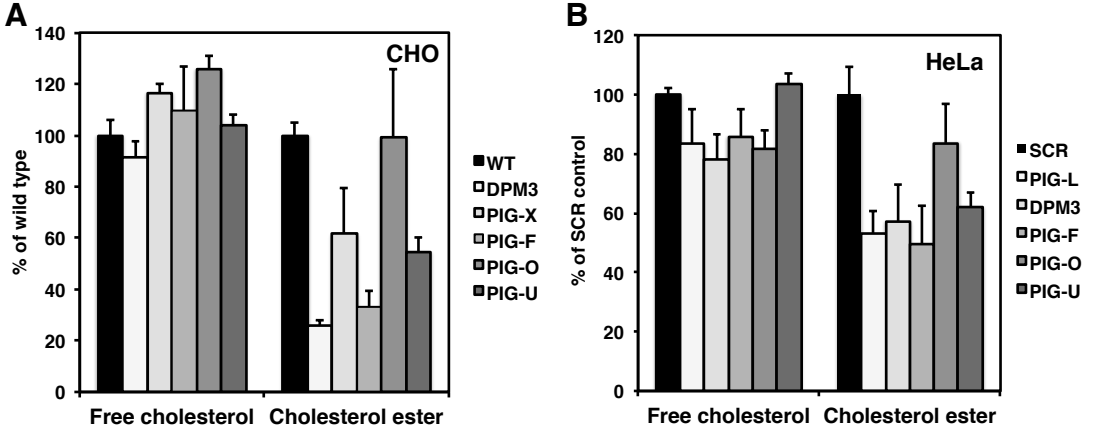
A
CHO
% of wild type
140
120
100
80
60
40
20
0
WT
DPM3
PIG-X
PIG-F
PIG-O
PIG-U
Free cholesterol
Cholesterol ester
B
HeLa
% of SCR control
120
100
80
60
40
20
0
SCR
PIG-L
DPM3
PIG-F
PIG-O
PIG-U
Free cholesterol
Cholesterol ester